Zoological Journal of the Linnean Society, 2018, **184**, 237–254. With 6 figures.

Morphological, ontogenetic and molecular data support strongylidiids as being closely related to Dorsomarginalia (Protozoa, Ciliophora) and reactivation of the family Strongylidiidae Fauré-Fremiet, 1961

XIAOTIAN LUO[1,2,3†], YING YAN[3,1†], CHEN SHAO[1*], SALEH A. AL-FARRAJ[4] WILLIAM A. BOURLAND[2] AND WEIBO SONG[3,5]

[1]*The Key Laboratory of Biomedical Information Engineering, Ministry of Education, School of Life Science and Technology, Xi'an Jiaotong University, Xi'an 710049, China*
[2]*Department of Biological Sciences, Boise State University, Boise, ID 83725, USA*
[3]*Institute of Evolution and Marine Biodiversity, Ocean University of China, Qingdao 266003, China*
[4]*Zoology Department, King Saud University, Riyadh 11451, Saudi Arabia*
[5]*Laboratory for Marine Biology and Biotechnology, Qingdao National Laboratory for Marine Science and Technology, Qingdao 266003, China*

Received 17 May 2017; revised 26 November 2017; accepted for publication 23 December 2017

Hypotrich ciliates, a large group of mainly free-living protists with highly diverse cortical structures, are commonly found in a broad variety of habitats worldwide. Methodological difficulties and insufficient faunistic studies have limited our understanding of their true biodiversity and phylogeny. In this report, two new *Strongylidium* species from China are investigated using live observation, protargol staining and 18S rRNA gene sequencing, and the evolution of strongylidiid ciliates is investigated based on morphological, morphogenetic and molecular data. Recently, the genera *Strongylidium* Sterki, 1878 and *Pseudouroleptus* Hemberger, 1985 were assigned to the family Spirofilidae Gelei, 1929. Given that these genera differ morphologically and phylogenetically from the type genus of Spirofilidae, *Hypotrichidium* Ilowaisky, 1921, their familial classification should be reconsidered. Moreover, the highly characteristic formation pattern of the mixed left ventral cirral row and other morphological features shared by *Strongylidium*, *Pseudouroleptus* and *Hemiamphisiella* Foissner, 1988, together with their 18S rRNA gene sequences, suggest that the three genera form a group closely related to Dorsomarginalia Berger, 2006. The family Strongylidiidae Fauré-Fremiet, 1961 is reactivated for these three genera.

ADDITIONAL KEYWORDS: *Hemiamphisiella* – *Pseudouroleptus* – Spirofilidae – Strongylidiidae – ***Strongylidium guangdongense* sp. nov.** – ***Strongylidium wuhanense* sp. nov**.

INTRODUCTION

The family Spirofilidae Gelei, 1929 is a group of hypotrichid ciliates with distinctly spiralled or obliquely curved cirral rows but unclear phylogenetic relationships, members of which occur in marine, brackish, limnetic and terrestrial habitats (Kahl, 1932; Paiva & Silva-Neto, 2007; Chen *et al.*, 2013a, b, 2015; Bourland, 2015). Lynn (2008) assigned 12 genera and one genus *incertae sedis*, *Kahliella* Tucolesco, 1962, to Spirofilidae. Recent studies have questioned the monophyly of Spirofilidae, and further investigation of the group's systematics and phylogeny is needed (Chen *et al.*, 2013a, b; Bourland, 2015).

Strongylidium Sterki, 1878, a genus assigned to the family Spirofilidae by Lynn (2008), has a long and complicated taxonomic history. Kahl (1932) defined *Strongylidium* as a genus with two spiralled marginal and two spiralled ventral cirral rows, a short tail-like or acute posterior body end, and no transverse cirri.

*Corresponding author. E-mail: andrews1201@hotmail.com
†These authors contributed equally
[Version of Record, published online 05 April 2018; http://zoobank.org/urn:lsid:zoobank.org:pub:BC0BABF3-C434-48D2-AD8C-929DB76C3FBD]

He compiled ten species of the genus, seven of which were previously unknown. After the monographic work by Kahl (1932), more species were added to the genus, making *Strongylidium* a heterogeneous group (Wang & Nie, 1932, 1935; Tucolesco, 1962; Foissner, 1982, 1987; Dragesco & Dragesco-Kernéis, 1986; Alekperov, 2005). Historically, *Strongylidium* has been classified within the families Oxytrichidae Ehrenberg, 1838 (Kahl, 1932; Corliss, 1961) and Strongylidiidae Fauré-Fremiet, 1961 (Stiller, 1975; Corliss, 1977, 1979; Jankowski, 1979). In the most recent major revisions, however, *Strongylidium* was placed within Spirofilidae, and Strongylidiidae was treated as a junior synonym of Spirofilidae (Tuffrau & Fleury, 1994; Shi, 1999; Lynn & Small, 2002; Jankowski, 2007; Lynn, 2008). Recently, Paiva & Silva-Neto (2007) redefined the genus and divided the species into five basic, informal groups, providing a clear and useful revision for further study of the genus *Strongylidium* as follows: 14 species possessing two marginal and two long ventral cirral rows, including the type species, were included in group I; and the other eight species were separated into groups II–V. However, few *Strongylidium* species have been investigated with modern techniques, and knowledge of the ciliature is still lacking for most species (Paiva & Silva-Neto, 2007; Chen *et al.*, 2013b). Additionally, data on divisional morphogenesis and molecular characterization are available for only two species of *Strongylidium* (Paiva & Silva-Neto, 2007; Chen *et al.*, 2013b). Therefore, in order to increase our understanding of the systematics and phylogeny of *Strongylidium*, morphological, morphogenetic and molecular studies from a wider range of isolates are needed. In the present study, we report details of the morphology, morphogenesis and phylogeny of two new species, namely *Strongylidium guangdongense* sp. nov. and *Strongylidium wuhanense* sp. nov., both from China.

MATERIAL AND METHODS

Collection, cultures and identification

Strongylidium guangdongense sp. nov. was isolated from samples collected from the Mangrove National Nature Reserve Park, Shenzhen (22°31′53″N, 114°00′34″E), Guangdong Province, southern China on 1 December 2015, from the sediment of a puddle containing a mixture of organic debris (Fig. 1A). The water temperature was 22 °C, and salinity was 7 practical salinity units. The raw cultures (ciliates are cultured with site water, excluding metazoans) from fresh

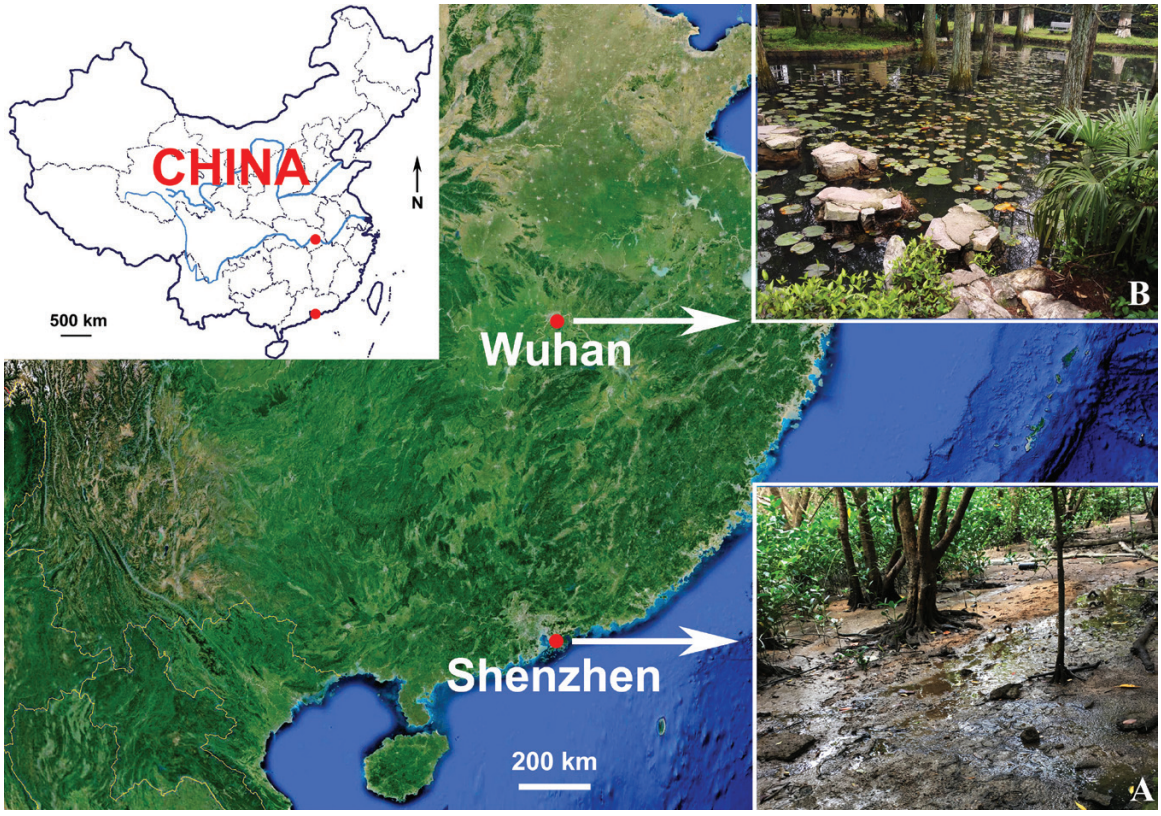

Figure 1. Photographs of the sample sites. A, a puddle in Shenzhen Mangrove National Nature Reserve (22°31′53″N, 114°00′34″E); B, a freshwater pond in Wuhan Botanical Garden, Chinese Academy of Science (30°32′57″N, 114°25′51″E).

samples were maintained in the laboratory for a week, during which time the cells were packed with ingested diatoms. All diatoms were digested ~10 h after isolation in filtered (0.22 μm) site water. Cells survived for only a short time (about a day) in filtered site water with rice for stimulation of bacterial growth, which indicates that the species is likely to live on diatoms.

Strongylidium wuhanense sp. nov. was isolated from samples collected on 8 April 2016 from a freshwater pond in Wuhan Botanical Garden, Chinese Academy of Science (30°32′57″N, 114°25′51″E), Hubei Province, China (Fig. 1B). The water temperature was 21 °C. *Strongylidium wuhanense* sp. nov. was collected using glass slides and sponges as artificial substrates submerged at a depth of 1 m to allow for colonization by ciliates. After 10 days, the artificial substrates were retrieved. The slides were transferred into Petri dishes containing unfiltered site water. Water from the sponges was squeezed gently into sample bottles. The raw cultures from the slides and sponge water were maintained in Petri dishes at 20 °C for 3 days. Subcultures that were kept in filtered (0.22 μm) site water or Eau de Volvic mineral water with rice to stimulate growth of bacteria for food failed.

Locomotion, contractility and cell shape were observed in the undisturbed live cells in Petri dishes. Live cells were isolated from raw cultures using micropipettes and observed with bright-field and differential interference contrast microscopy. The protargol staining followed the protocol of Wilbert (1975), and the protargol was made according to Pan, Bourland & Song (2013). In protargol preparations, the stained specimens swelled and the tail contracted. The cells used for protargol staining were isolated from the raw cultures or starved in filtered site water for ~10 h. *In vivo* measurements were taken at ×100 to ×1000 magnification. Counts and measurements of the stained specimens were conducted at ×1000 magnification. The stained specimens were drawn at a magnification of ×1250, with the help of a drawing attachment and photomicrographs. In drawings of the morphogenetic stages, parental cirri are shown as outlines and newly formed ones are filled in. Terminology is according to Paiva & Silva-Neto (2007).

DNA extraction, gene sequencing and phylogenetic analyses

DNA extraction was performed with the DNeasy Blood & Tissue Kit (Qiagen, Valencia, CA, USA). PCR amplification and sequencing of the 18S rRNA gene were performed according to Zhao *et al.* (2015). The Euk A and Euk B primers were used for 18S rRNA gene amplification (Medlin *et al.*, 1988). The PCR products were sequenced at the Tsingke sequencing centre (Qingdao, China) using primers Euk A and Euk B and three internal primers (Wang *et al.*, 2016).

All additional sequences for constructing the phylogenetic trees were downloaded from the National Center for Biotechnology Information (NCBI) Database. All sequences were aligned in GUIDANCE 2. Ambiguous columns (confidence score of < 0.358) were removed using the GUIDANCE 2 Web server (Sela *et al.*, 2015). The final alignment included 1794 sites and 80 taxa. Four oligotrichous ciliates, *Novistrombidium orientale*, *Parastrombidinopsis minima*, *Strombidinopsis acuminata* and *Strombidium apolatum*, were selected as outgroup taxa. Maximum likelihood (ML) analysis, with 1000 bootstrap replicates, was carried out using RAxML-HPC2 on XSEDE v. 8.2.9 (Stamatakis, 2014) on the CIPRES Science Gateway V. 3.3 (URL: http://www.phylo.org; Miller, Pfeiffer & Schwartz, 2010). The DNA partition was analysed using the general time reversible + gamma model (Gao *et al.*, 2016). Bayesian inference analysis was performed with MrBayes on XSEDE 3.2.6 (Ronquist *et al.*, 2012) on the CIPRES Science Gateway V. 3.3 (URL: http://www.phylo.org) using the general time reversible + invariable sites + gamma model selected by the program MrModeltest v.3.4 according to the Akaike information criterion (Nylander, 2004). Parameters of Bayesian analysis included two runs with four chains and 10 000 000 generations sampled every 100 generations, with the initial 25 000 trees discarded as burn-in. The remaining trees were used to calculate the posterior probabilities with a majority-rule consensus. The tree topologies were visualized using MEGA 6.0 (Tamura *et al.*, 2013). The systematic classification follows Paiva & Silva-Neto (2007), Lynn (2008) and Adl *et al.* (2012).

RESULTS

Subclass Hypotrichia Stein, 1859

Family Strongylidiidae Fauré-Fremiet, 1961

Genus *Strongylidium* Sterki, 1878

***Strongylidium guangdongense* sp. nov.**

(Figs 2–4; Table 1)

urn:lsid:zoobank.org:act:157A624A-F01B-4D29-9823-D0D4F30D8329

Diagnosis: Body ~100–150 μm × 40–50 μm *in vivo*; cell outline more or less fusiform, with rounded anterior end and inconspicuous tail; cortical granules colourless, spherical, ~1–1.5 μm across; ~30 adoral membranelles; three frontal, one buccal, one postoral ventral, usually one frontoventral cirrus; two long ventral cirral rows, averaging 34 and 32 in left and right rows, respectively; 29 left and 35 right marginal

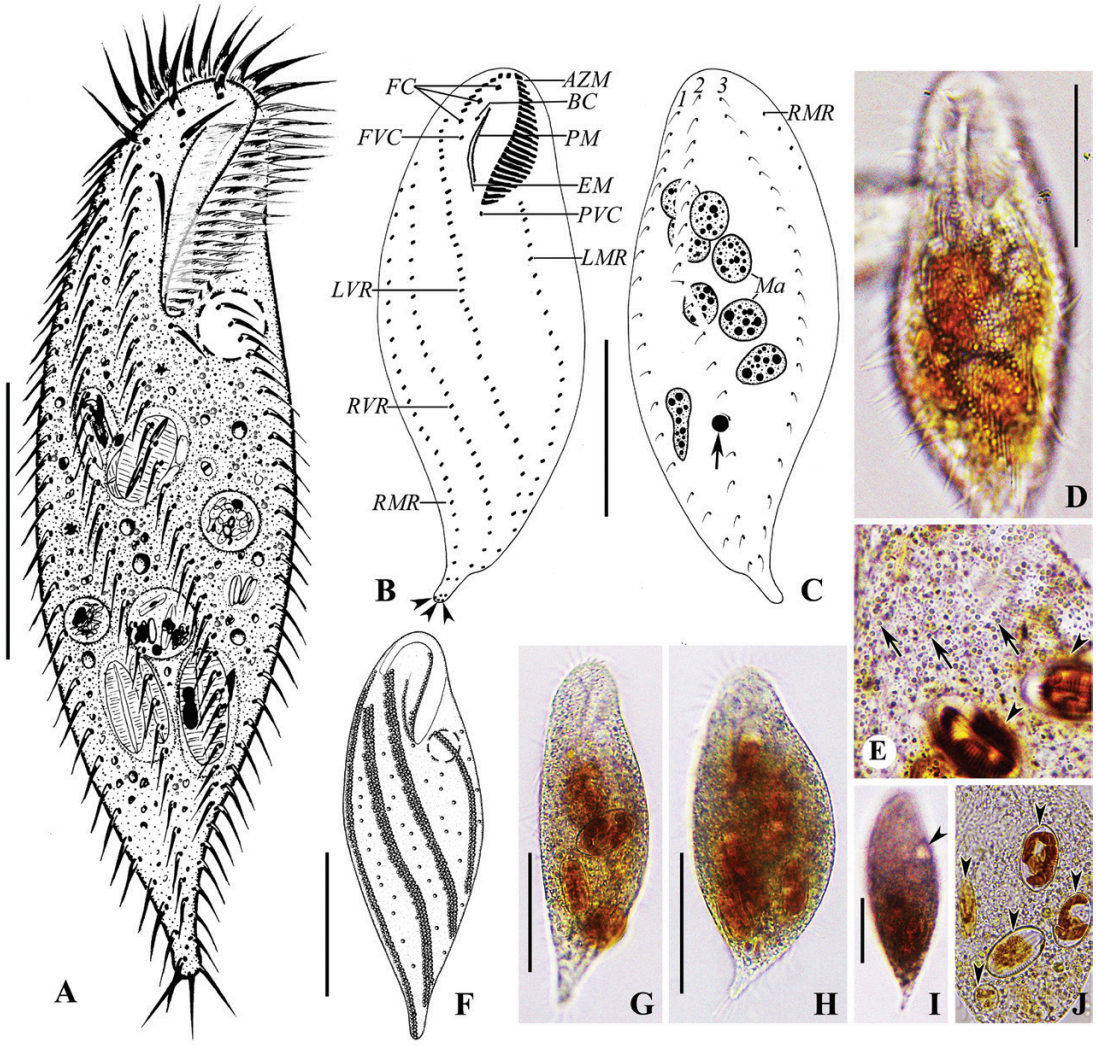

Figure 2. ***Strongylidium guangdongense*** **sp. nov.** live (A, D–J) and after protargol staining (B, C). A, ventral view of a representative specimen. B, C, ventral (B) and dorsal (C) views of holotype, showing infraciliature and nuclear apparatus. Arrowheads mark caudal cirri; arrow indicates micronucleus. D, ventral view, showing the slightly oblique sigmoid ventral cirral rows and cortical granules distributed along cirral rows. E, cortical granules (arrows) and algae in food vacuoles (arrowheads). F, ventral view, showing the distribution of cortical granules. G–I, ventral views of representative individuals, showing body shape and contractile vacuole (arrowhead). J, various kinds of algae (arrowheads). AZM, adoral zone of membranelles; BC, buccal cirrus; EM, endoral membrane; FC, frontal cirri; FVC, frontoventral cirrus; LMR, left marginal cirral row; LVR, left ventral cirral row; Ma, macronuclear nodules; PM, paroral membrane; PVC, postoral ventral cirrus; RMR, right marginal cirral row; RVR, right ventral cirral row; 1–3, dorsal kineties. Scale bars: 50 μm.

cirri; three dorsal kineties; three caudal cirri; about eight macronuclear nodules; brackish water habitat.

Type locality and ecology: Mangrove National Nature Reserve Park, Shenzhen (22°31′53″N, 114°00′34″E), China.

Type specimens: A protargol slide containing the holotype specimen (see Figs 2B, C, 3A, B; registration no. LXT2015120101/1) and five paratype slides (registration no. LXT2015120101/2–6) were deposited in the Laboratory of Protozoology, Ocean University of China.

Etymology: The species-group name *guangdongense* refers to the area (Guangdong) from which the species was collected.

Morphology: Body 100–150 μm × 40–50 μm *in vivo*, somewhat fusiform in shape, with rounded anterior end and tapered posterior end, with inconspicuous tail,

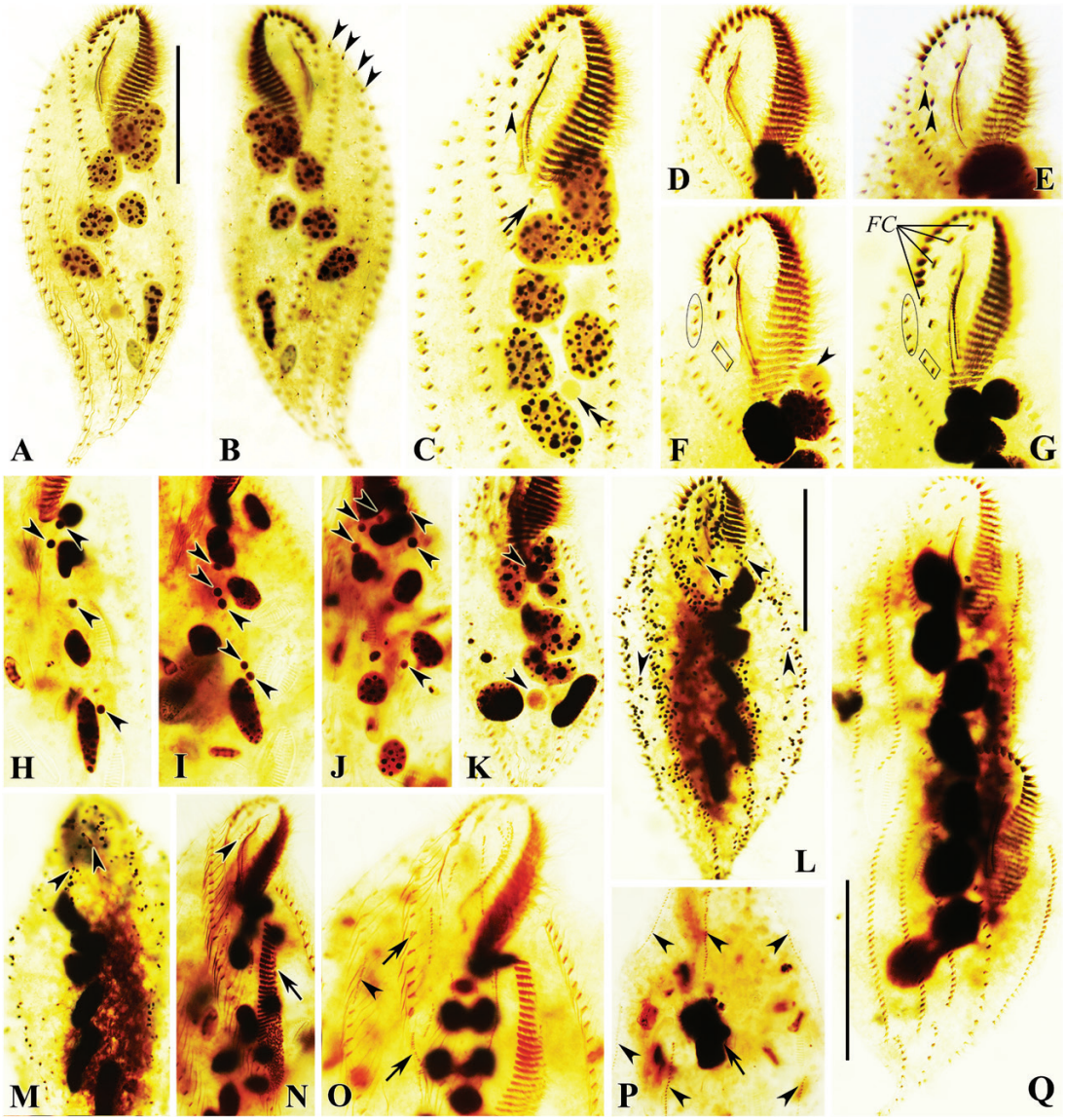

Figure 3. ***Strongylidium guangdongense*** **sp. nov.** after protargol staining. A, B, ventral (B) and dorsal (C) views of holotype, showing infraciliature and nuclear apparatus. Arrowheads mark several anterior-most right marginal cirri on dorsal surface. C–E, specimens with one (C), zero (D) and two (E) frontoventral cirri (arrowheads). Arrow marks the postoral ventral cirrus; double arrowhead indicates the micronucleus. F, G, specimens with cirri in left ventral cirral row not arranged in a typical row. Ovals indicate the anterior segment; rectangles mark the median segment; and arrowhead marks the large-sized micronucleus. H–K, various sizes and numbers of micronuclei (arrowheads); raw cultured specimens with smaller and more micronuclei (H–J), and starved specimens with larger and fewer micronuclei (K). L, M, cortical granules arranged along cirral rows and dorsal kineties on ventral (L) and dorsal (M) sides. Arrowheads show hair-like extruded cortical granules. N, ventral view of an early divider, showing the dedifferentiated buccal cirrus (arrowhead) and the newly formed adoral membranelles (arrow). O, ventral view of an early-middle divider. Arrows indicate frontal-ventral-transverse cirral anlagen V of both dividers, and arrowhead shows frontal-ventral-transverse cirral anlage VI of proter. P, dorsal view of a middle divider, showing dorsal kineties anlagen (arrowheads) and the completely fused macronuclear mass (arrow). Q, ventral view of a late divider. FC, frontal cirri. Scale bars: 50 μm.

flexible, only slightly contractile (Fig. 2A, G–I). Ratio of length to width ~5:2–3:1, dorsoventrally flattened ~3:2. Macronucleus left of cell median, composed of four to 12, averaging eight, globular to ellipsoidal nodules. One to seven globular micronuclei near, or adjacent to, macronuclear nodules, ~2–8 μm across, usually one or

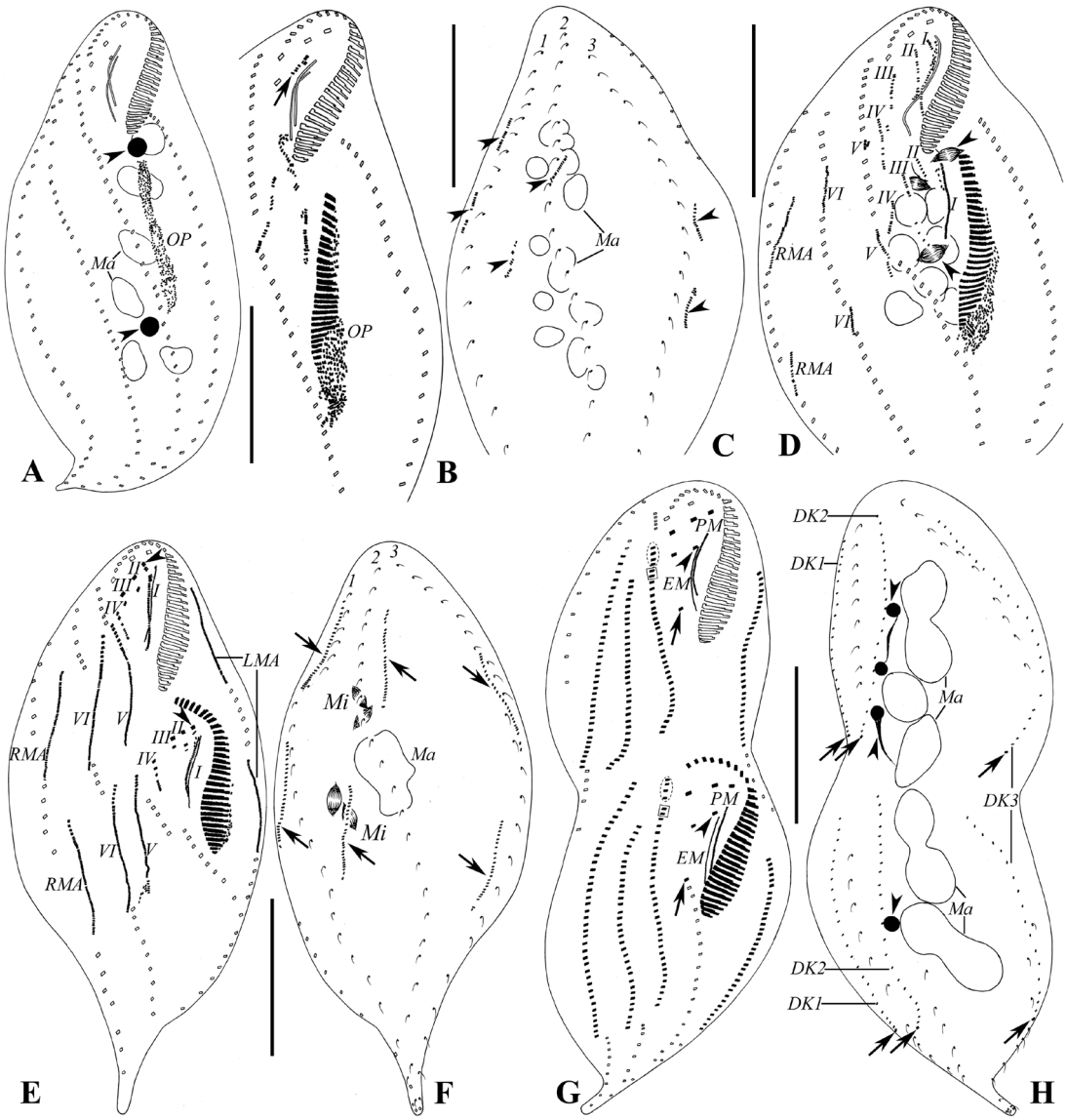

Figure 4. Morphogenesis of ***Strongylidium guangdongense* sp. nov.** after protargol staining. A, ventral view of a very early divider, showing oral primordium of the opisthe. Arrowheads mark micronuclei. B, C, ventral (B) and dorsal (C) views of an early divider. Arrow indicates the dedifferentiated buccal cirrus, and arrowheads show the newly formed dorsal kineties anlagen. D, ventral view of an early-middle divider, showing all the frontal-ventral-transverse cirral anlagen (FVTA) and the right marginal anlagen. Arrowheads mark micronuclei. E, F, ventral (E) and dorsal (F) views of a middle divider. Arrowheads mark the newly formed left frontal cirri, and arrows indicate dorsal kineties anlagen. G, H, ventral (G) and dorsal (H) views of a late divider, showing the migration of the newly formed cirri. Arrowheads in (G) indicate buccal cirri; arrows in (G) mark postoral ventral cirri; dashed circles and squares in (G) indicate the anterior and the median segment of the left ventral cirral row, respectively; arrowheads in (H) indicate micronuclei; and arrows in (H) show caudal cirri. DK1–DK3, new dorsal kineties; EM, new endoral membrane; LMA, left marginal cirral anlage; Ma, macronuclear nodules; Mi, micronuclei; OP, oral primordium of the opisthe; PM, new paroral membrane; RMA, right marginal cirral anlage; I–VI, frontal-ventral-transverse cirral anlagen; 1–3, parental dorsal kineties. Scale bars: 50 μm.

two larger-sized (3–8 μm, on average 4 μm) micronuclei in starved cells, four to seven smaller-sized (2–3 μm) micronuclei in raw cultured cells after protargol staining (Figs 2C, 3C, H–K). One contractile vacuole ~12 μm in diameter in diastole, about at level of cytostome near left margin of body (Fig. 2A, I). Cortical granules colourless, spherical, ~1–1.5 μm across, arranged in longitudinal rows along cirral rows and dorsal

Table 1. Morphometric characterization of ***Strongylidium guangdongense* sp. nov.** (upper line) and ***Strongylidium wuhanense* sp. nov.** (lower line) based on protargol-stained specimens (measurements in micrometres)

Character	Minimum	Maximum	Mean	Median	SD	CV	*N*
Body, length	107	188	157.1	159.0	21.9	13.9	23
	134	185	160.5	161.0	13.7	8.6	15
Body, width	44	75	59.3	61.0	7.4	12.5	23
	47	78	61.9	63.0	9.9	16.0	15
Body width-to-length ratio	32	46	38.0	37.7	3.6	9.4	23
	31	46	38.5	38.9	4.7	12.3	15
Adoral zone, length	32	49	41.5	42.0	3.7	8.9	23
	32	46	40.2	41.0	4.5	11.3	15
Adoral zone-to-body length ratio	24	30	26.6	26.6	2.1	7.8	23
	18	29	25.1	25.4	3.0	11.8	15
Adoral membranelles, number*	25	34	30.8	31.0	2.4	7.8	23
AZM1, number†	5	9	7.3	8.0	1.4	19.8	15
AZM2, number†	15	23	20.9	22.0	2.4	11.6	15
Frontal cirri, number	3	4	3.1	3.0	0.3	11.0	23
	2	3	2.9	3.0	0.4	12.3	15
Buccal cirrus, number	1	1	1.0	1.0	0	0	23
	1	1	1.0	1.0	0	0	15
Frontoventral cirri, number	0	2	1.1	1.0	0.4	38.4	23
	0	1	0.9	1.0	0.3	28.8	14
Postoral ventral cirrus, number	1	1	1.0	1.0	0	0	14
	1	1	1.0	1.0	0	0	13
Left ventral cirri, number	29	39	34.1	34.5	3.5	10.2	18
	30	49	39.6	40.0	5.1	12.8	14
Right ventral cirri, number	24	38	31.9	30.0	4.0	12.4	22
	34	48	37.9	35.5	5.2	13.6	14
Left marginal cirri, number	21	36	29.3	29.0	3.9	13.2	16
	31	48	38.9	40.0	5.1	13.1	14
Right marginal cirri, number	25	48	35.0	35.0	5.8	16.5	21
	34	45	40.7	43.0	3.6	8.9	15
Caudal cirri, number	3	3	3.0	3.0	0	0	23
	3	3	3.0	3.0	0	0	15
Dorsal kineties, number	3	3	3.0	3.0	0	0	23
	3	3	3.0	3.0	0	0	15
Bristles of dorsal kinety 1, number	16	27	19.4	18.5	3.3	17.0	8
	30	38	32.9	33.0	2.6	7.8	12
Bristles of dorsal kinety 2, number	12	26	18.6	18.5	3.9	20.7	8
	27	37	30.6	29.0	3.2	10.4	9
Bristles of dorsal kinety 3, number	12	25	18.8	18.5	3.7	19.7	8
	26	36	30.8	30.5	3.6	11.7	10
Macronuclear nodules, number	4	12	7.5	8.0	1.7	23.0	29
	15	19	16.1	16.0	1.1	6.6	15
Length of macronuclear nodule‡	9	32	17.6	17.0	5.7	32.6	29
	7	14	9.1	9.0	2.2	23.8	15
Width of macronuclear nodule‡	6	19	11.9	12.0	2.9	24.5	29
	5	10	6.6	6.0	1.6	24.8	15
Length of macronuclear nodule§	6	15	10.7	11.0	2.3	21.1	29
	5	10	5.7	5.0	1.3	23.7	15
Width of macronuclear nodule§	6	12	9.1	9.0	1.7	18.9	29
	3	9	5.0	5.0	1.4	27.3	15

Table 1. *Continued*

Character	Minimum	Maximum	Mean	Median	SD	CV	*N*
Micronuclei, number	1	7	2.5	2.0	1.9	73.9	19
	2	2	2.0	2.0	0	0	14
Length of micronuclei	2	8	4.3	4.0	1.5	34.6	19
	4	6	4.8	5.0	0.6	12.1	14

Abbreviations: AZM1, distal part of adoral zone of membranelles; AZM2, proximal part of adoral zone of membranelles; CV, coefficient of variation expressed as a percentage; mean, arithmetic mean; *N*, number of specimens examined.
*Data for ***Strongylidium guangdongense*** **sp. nov.**
†Data for ***Strongylidium wuhanense*** **sp. nov.**
‡Data for the largest macronuclear nodule.
§Data for the smallest macronuclear nodule.

kineties, irregularly distributed between cirral rows and dorsal kineties, easily stained with protargol, and some granules extruded, forming hair-like structures on the cell surface in protargol-stained specimens (Figs 2D–F, 3L, M). Cytoplasm colourless, packed with food vacuoles containing numerous diatoms, usually present in middle region of cell, rendering cells slightly brownish in appearance at low magnification (Fig. 2E, G–J). Cells crawl slowly on substrate and among debris in the bottom of Petri dishes.

Usually three, rarely four moderately enlarged frontal cirri (Fig. 3C–G), rightmost just behind distal end of adoral zone, with cilia ~12–15 μm long *in vivo*. All other cirri ~8–10 μm long, except for the caudal cirri (10–12 μm; Fig. 2A, D). Invariably one buccal, one postoral ventral cirrus and usually one, sometimes two frontoventral cirri, rarely absent (three out of 23 specimens analysed having two frontoventral cirri, only one cell with no frontoventral cirri; Figs 2B, 3C–E). Two long, slightly oblique, sigmoid ventral cirral rows. Left ventral cirral row commences approximately near rightmost frontal cirrus, comprising 29–39 cirri, terminated at ~80% of cell length. Anterior, middle and posterior parts of left ventral cirral row generated from anterior segments of frontal-ventral-transverse cirral anlage (FTVA) VI and IV and whole of V, with cirri of the three parts usually arranged in a typical row (Fig. 3A, C–E); occasionally, cirri from anlage VI located slightly left of the row (Fig. 3F, G). Right ventral cirral row starts near level of posterior third of buccal cavity, ends slightly subterminally, comprising 24–38 cirri. Left and right marginal cirral rows both reach posterior end of cell, composed of 21–36 and 25–48 cirri, respectively; several anteriormost right marginal cirri reach dorsal surface (Figs 2B, C, 3A, B). Three dorsal kineties extend almost entire length of cell, one caudal cirrus at end of each dorsal kinety (Figs 2A–C, 3B), dorsal bristles ~3 μm long *in vivo*.

The adoral zone occupied ~27% of body length after protargol staining. Adoral zone is composed of 25–34 membranelles, with cilia ~15–18 μm long *in vivo*. Bases of membranelles are unequal in length, those in distal part comprising three short, equal-length rows of kinetosomes, those in proximal part with four rows, one short and three long (Figs 2B, 3C). Buccal cavity narrow, with right margin of cavity in midline (Fig. 2A, D). Paroral and endoral membranes more or less in *Oxytricha* pattern, almost equal in length, slightly curved, optically intersect near anterior end of the latter (Figs 2B, 3A, C–G). Endoral membrane comprising single row of kinetosomes, starting at level of buccal cirrus. Paroral with multiple rows of kinetosomes, begins slightly anterior to endoral (Figs 2B, 3A, C–G).

Morphogenesis: Stomatogenesis commences with the formation of the oral primordium of the opisthe, a longitudinal field of closely spaced basal bodies behind the parental adoral zone of the membranelles, between the left ventral cirral row and the left marginal cirral row (Fig. 4A). Parental cirri do not contribute to formation of the oral primordium.

In an early divider (Figs 3N, 4B), basal bodies for the oral primordium proliferate and differentiate into new membranelles, beginning at the anterior portion and progressing posteriorly. At the same time, in the opisthe, the undulating membrane anlage appears to the right of the oral primordium. The parental postoral ventral cirrus disappears and may contribute to the formation of the FVTA but may also simply be resorbed. Another FTVA (probably FVTA V) originates from the left ventral cirral row. Simultaneously, in the proter, the parental buccal cirrus (II/1) begins to dedifferentiate into FVTA II.

In an early middle divider (Figs 3O, 4D), all the FVTA have formed. In the proter, the undulating membrane anlage is formed from the old undulating membranes, and the FVTA III originates from the parental frontoventral cirrus. For both the proter and opisthe, the left and right ventral cirral rows dedifferentiate and intrakinetally form FTVA V and VI, respectively. However, some key stages were not observed, so the origins of the other FVTA are not clear.

In the middle stage (Fig. 4E), the undulating membrane anlagen splits longitudinally into paroral and endoral

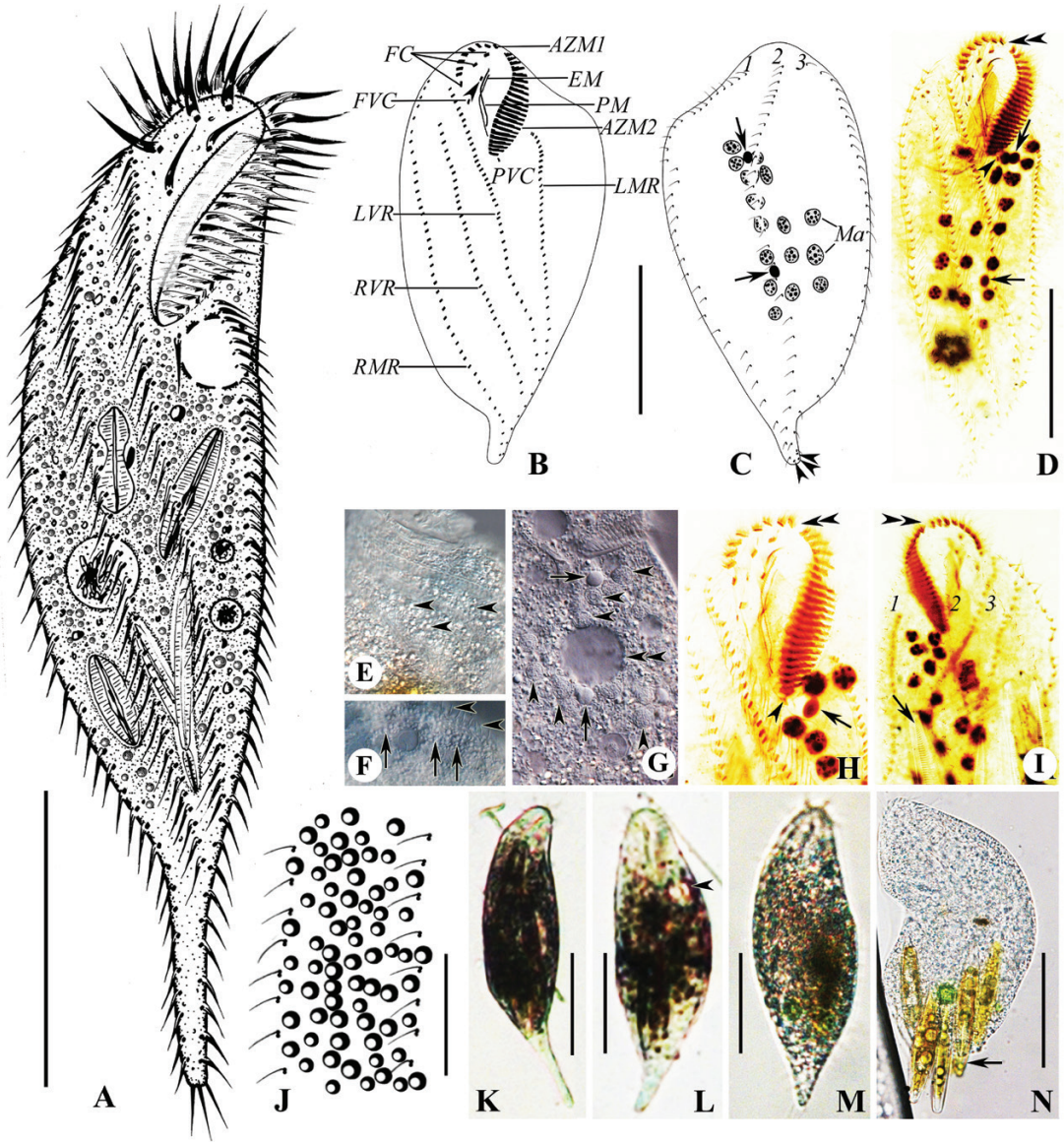

Figure 5. ***Strongylidium wuhanense*** **sp. nov.** live (A, E–G, J–N) and after protargol staining (B–D, H, I). A, ventral view of a representative specimen. B–D, ventral (B, D) and dorsal (C) views of holotype, showing infraciliature and nuclear apparatus. Arrowhead in (B) indicates buccal cirrus; arrowheads in (C) mark caudal cirri; arrowhead in (D) marks the postoral ventral cirrus; double arrowhead shows the gap between two parts of adoral zone of membranelles; and arrows mark micronuclei. E, ventral view, showing the shining granules (arrowheads). F, dorsal side, showing dorsal bristles (arrowheads) and cortical granules (arrows). G, ventral view, showing macronuclear nodules (arrowheads), two large micronuclei (arrows), and contractile vacuole (double arrowhead). H, I, ventral (H) and dorsal (I) views of anterior part. Double arrowheads indicate the gap between two parts of adoral zone of membranelles; arrowhead marks the postoral ventral cirrus; arrow in (H) marks the large micronucleus; and arrow in (I) shows the diatom. J, dorsal view, showing the distribution of cortical granules. K–M, ventral views of representative individuals, showing body shape and contractile vacuole (arrowhead). N, a heavily squeezed cell, showing the diatoms (arrow). AZM1, distal part of adoral zone of membranelles; AZM2, proximal part of adoral zone of membranelles; EM, endoral membrane; FC, frontal cirri; FVC, frontoventral cirrus; LMR, left marginal cirral row; LVR, left ventral cirral row; Ma, macronuclear nodules; PM, paroral membrane; PVC, postoral ventral cirrus; RMR, right marginal cirral row; RVR, right ventral cirral row; 1–3, dorsal kineties. Scale bars: 50 μm.

membranes, which give rise to the leftmost frontal cirrus in both proter and opisthe. All FVTA lengthen to long streaks and begin to differentiate into new cirri.

In the late stage (Figs 3Q, 4G), the FVTA differentiate into new cirri, which migrate to their final position in both the proter and the opisthe: FVTA II gives rise

to the middle frontal cirrus and the buccal cirrus; FVTA III contributes to the rightmost frontal and usually one frontoventral cirrus; FVTA IV differentiates into one postoral ventral cirrus and probably two cirri of the middle part of the left ventral cirral row; cirri originating from FVTA V form the posterior part of the left ventral cirral row; and FVTA VI contributes to the whole right ventral cirral row and the anterior part of left ventral cirral row.

The marginal cirral row anlagen develop intrakinetally through dedifferentiation of the parental cirri (Fig. 4D, E). Then, all anlagen lengthen towards both ends of the dividing cell while the parental cirri are resorbed (Fig. 4G). Dorsal kinety anlagen (DKA) originate *de novo* (Figs 3P, 4C, F). In the late stage, one caudal cirrus is formed at the posterior end of each DKA (Fig. 4H).

All macronuclear nodules fuse into a single mass and then divide (Fig. 4A, C, D, F, H).

STRONGYLIDIUM WUHANENSE SP. NOV.

(FIG. 5; TABLE 1)

urn:lsid:zoobank.org:act:6A330535-8F81-4766-9F0C-C3B4C1CE8E13

Diagnosis: Freshwater *Strongylidium*; 135–200 μm × 40–60 μm *in vivo*; cell with a conspicuous tail; cortical granules colourless, spherical, ~1–1.5 μm across, irregularly distributed; adoral zone more or less bipartite, with approximately seven distal and 21 proximal membranelles; three frontal, one buccal, one postoral ventral, usually one frontoventral cirrus; two long ventral cirral rows, average of 40 and 38 cirri on left and right row, respectively; 39 left and 41 right marginal cirri; three dorsal kineties; three caudal cirri; ~16 macronuclear nodules, invariably two micronuclei.

Type locality and ecology: Wuhan Botanical Garden, Wuhan (30°32′57′′N, 114°25′51′′E), China. Water temperature 21 °C.

Type specimens: A protargol slide containing the holotype specimen (see Fig. 5B–D; registration no. LXT2016040803/1) and three paratype slides (registration no. LXT2016040803/2–4) were deposited in the Laboratory of Protozoology, Ocean University of China.

Etymology: The species-group name *wuhanense* refers to the location (Wuhan) where the species was discovered.

Morphology: Body 135–200 μm × 40–60 μm *in vivo*, more or less fusiform in shape, with anterior end rounded. Tail conspicuous, highly contractile, about one-fifth to one-quarter of body length when fully extended in Petri dishes (Fig. 5K), indistinct when contracted (Fig. 5L, M). Ratio of length to width ~3–4:1, dorsoventrally flattened ~3:2 (Fig. 5A, K–M). Macronucleus slightly left of cell median, composed of 15–19, averaging 16, small-sized (the biggest 7 μm × 9 μm on average; the smallest 5 μm × 6 μm on average) globular to ellipsoidal nodules. Invariably two globular to ellipsoidal micronuclei, near macronuclear nodules, ~4–6 μm across, only slightly smaller than macronuclear nodules (Fig. 5C, D, G, H). One contractile vacuole ~12 μm across in diastole, near left margin of body about at level of cytostome (Fig. 5A, G, L). Cortex flexible. Cortical granules, colourless, spherical, ~ 1–1.5 μm across, irregularly distributed throughout the cortex dorsally (Fig. 5F, J). Cytoplasm colourless, middle region of cell usually packed with numerous shining granules (~1–3 μm diameter) and food vacuoles containing various algae (Fig. 5E, I, N), rendering cells opaque and with a dark appearance at low magnification (Fig. 5K–M). Cells crawl slowly on substrate and among debris.

Cilia of cirri ~8–10 μm long *in vivo*, except for three moderately enlarged frontal cirri, ~12–15 μm in length. Invariably one buccal and one postoral ventral cirrus. Usually one frontoventral cirrus (one out of 14 specimens analysed having no frontoventral cirrus). Two long, slightly obliquely arranged ventral cirral rows, both extending subterminally. Left ventral cirral row beginning about at level of rightmost frontal cirrus, comprising 30–49 cirri; right ventral cirral row with 34–48 cirri, starting near level of posterior third of buccal cavity. Left and right marginal cirral rows both reaching to posterior end of cell, composed of 31–48 and 34–45 cirri, respectively (Fig. 5B, D). Three bipolar dorsal kineties with dorsal bristles ~3 μm long *in vivo* and closely spaced (Fig. 5C, F, I). Three caudal cirri (10–12 μm long *in vivo*) positioned at the tip of tail, inconspicuous and not distinguishable from marginal cirri (Fig. 5A, C).

Adoral zone occupied ~25% of body length in protargol-stained specimens. Buccal cavity narrow, with right margin of cavity near cell midline. Adoral zone slightly bipartite, with inconspicuous gap between distal and proximal parts comprising five to nine and 15–23 membranelles, respectively (Fig. 5D, H, I). Bases of membranelles in distal part comprising three short, equal-length rows of kinetosomes, and those in proximal part containing four rows, one short and three long (Fig. 5B, D). Undulating membranes more or less in *Oxytricha* pattern, almost equal in length, slightly curved and optically intersecting in middle part; paroral multiple rowed, commences slightly ahead of single-rowed endoral (Fig. 5B, D, H).

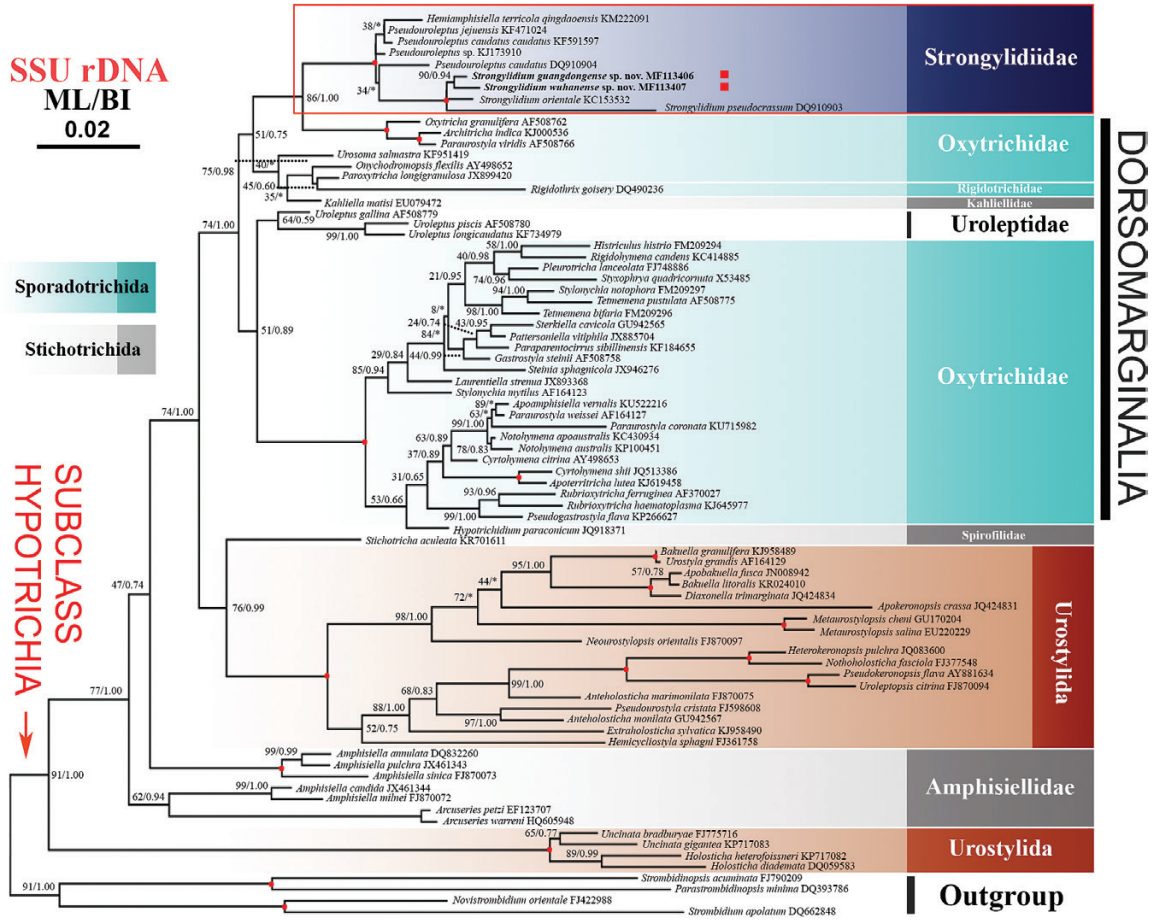

Figure 6. The maximum likelihood (ML) tree inferred from 18S rRNA gene sequences, showing the position of the new species ***Strongylidium guangdongense* sp. nov.** and ***Strongylidium wuhanense* sp. nov.** (in bold). Numbers at nodes represent the bootstrap values of maximum likelihood analysis and the posterior probability of Bayesian analysis. Fully supported (1.00/100) branches are marked with filledd circles. Asterisk indicates the disagreement between Bayesian inference tree and the reference ML tree. All branches are drawn to scale. Scale bar corresponds to two substitutions per 100 nucleotide positions.

18S rRNA gene sequence and phylogenetic analyses

(Fig. 6)

The partial sequence of the 18S rRNA gene of *Strongylidium guangdongense* sp. nov. (GenBank accession number: MF113406) is 1670 bp long and has a G + C content of 45.15%. In *Strongylidium wuhanense* sp. nov. (GenBank accession number: MF113407) the gene is 1696 bp long and has a G + C content of 45.11%.

The nodes from the topologies generated with ML and BI were generally concordant (Fig. 6). As described in previous studies (Chen *et al.*, 2016, 2017; Dong *et al.*, 2016; Huang *et al.*, 2016; Kumar *et al.*, 2016; Li *et al.*, 2016, 2017; Luo *et al.*, 2016, 2017; Park *et al.*, 2017), 18S rRNA gene sequences from Stichotrichida and Sporadotrichida intermingle, and neither order is monophyletic. The family Spirofilidae *sensu* Lynn (2008) is not monophyletic, as the type genus *Hypotrichidium* nests in the large group of oxytrichids. *Stichotricha aculeata* branched as sister to 'core urostylids', and *Strongylidium* species fell within the *Strongylidium–Hemiamphisiella–Pseudouroleptus* group, which is fully supported (ML/BI, 100/1.00). The genus *Strongylidium* formed a fully supported monophyletic group (ML/BI, 100/1.00) with the new species, *Strongylidium guangdongense* sp. nov. and *S. wuhanense* sp. nov., nested inside.

DISCUSSION

Establishment of two new species

In the comprehensive revision of *Strongylidium* by Paiva & Silva-Neto (2007), the 22 morphological species originally assigned to the genus were divided into five groups. Together with the type species

Strongylidium crassum Sterki, 1878, 14 congeners were assigned to group I, characterized by the possession of two long ventral and two marginal cirral rows. Owing to their infraciliature, *S. guangdongense* sp. nov. and *S. wuhanense* sp. nov. should be included in this group. After redefinition of *Strongylidium* by Paiva & Silva-Neto (2007), another species, *Strongylidium orientale* Chen *et al.*, 2013, was added to the genus. Among the 15 species of the genus *Strongylidium* in group I, only *Strongylidium muscorum* Kahl, 1932, *Strongylidium californicum* Kahl, 1932, the marine form *Strongylidium* sp. (Kahl, 1932), and probably *Strongylidium lentum* (Biernacka, 1963) Paiva & Silva-Neto, 2007 have multiple macronuclear nodules like *S. guangdongense* sp. nov. and *S. wuhanense* sp. nov. Therefore, the species we have described differ from others with only two macronuclear nodules. When compared with all the species having multiple macronuclear nodules, *S. guangdongense* sp. nov. and *S. wuhanense* sp. nov. are two new distinctive members of the genus *Strongylidium* (Table 2).

Morphogenetic comparison with congeners

Morphogenetic characters have never been documented in the type species of *Strongylidium*, *S. crassum*, a little known and only briefly characterized taxon. We were unable to detail morphogenesis in *S. wuhanense* sp. nov. owing to insufficient material.

Paiva & Silva-Neto (2007) described the morphogenetic process for the first time in a congener, *Strongylidium pseudocrassum*, and Chen *et al.* (2013b) detailed the ontogenetic process of a new species, *S. orientale*. During cell division, there are some minor differences between them, as follows: (1) during division, the parental adoral zone remained complete in *S. guangdongense* sp. nov. and *S. pseudocrassum*, but the posterior part of the adoral zone was renewed by dedifferentiation in *S. orientale*; (2) the undulating membrane anlage for the proter came from the old undulating membranes in *S. guangdongense* sp. nov. and *S. orientale*, but developed from a long streak of basal bodies originating from the distal end of the undulating membrane primordium of the opisthe in *S. pseudocrassum*; and (3) the FVTA V arose independently in each divider in *S. guangdongense* sp. nov. and *S. orientale*, whereas the FVTA V originated as a long primary streak in *S. pseudocrassum*, extending parallel to the right side of the parental left ventral cirral row and then fragmenting in two secondary primordia. However, *S. guangdongense* sp. nov. still shows high similarity to both congeners, as follows: (1) the oral primordium in the opisthe occurs *de novo* at the cell surface; (2) the left ventral cirral row is formed from

Table 2. Morphometrical and morphological comparison of six *Strongylidium* species with multiple macronuclear nodules (measurements in micrometres)

Character	***S. guangdongense* sp. nov.**	***S. wuhanense* sp. nov.**	*S. muscorum*	*S. californicum*	*S. lentum*	*Strongylidium* sp.
Size *in vivo*	100–150 × 40–50	135–200 × 40–60	100–110	250	120–150 × 25	70
General body shape	Fusiform, with an inconspicuous tail	Fusiform, with a conspicuous tail	Smoothed slightly from front to rear; rear end rounded	Very slender conical; rear end rounded	Slender fusiform, with a distinct tail	Slightly pointed at rear end
Tail	Inconspicuous	Conspicuous	Non-existent	Non-existent	Conspicuous	Non-existent
Gap in AZM	Non-existent	Existent	Non-existent	Non-existent	Non-existent	Existent
Cirral rows	Slightly spiralled	Slightly spiralled	Slightly spiralled	Heavily spiralled	Heavily spiralled	Slightly spiralled
Cirri in frontal area, number	5	5	4	4–5	5	3
Ma, number	4–12	15–19	Numerous	~30	–	4–5
Mi, number	2	2	–	4	–	–
Habitat	Brackish	Freshwater	Freshwater	Freshwater	Marine/ brackish	Marine
Data source	Present work	Present work	Kahl (1932)	Kahl (1932)	Kahl (1932); Biernacka (1963)	Kahl (1932)

Abbreviations: AZM, adoral zone of membranelles; Ma, macronuclear nodules; Mi, micronuclei; characters with '–' are not available from the source cited.

three parts, with the anterior, middle and posterior part coming from the anterior segments of FVTA VI and IV and the whole of FVTA V, respectively; (3) the right ventral cirral row dedifferentiates intrakinetally into FVTA VI in both dividers; (4) the marginal rows develop intrakinetally; (5) the dorsal kineties replicate entirely *de novo*, and there is no dorsal kinety fragmentation or dorsomarginal kineties present; and (6) one caudal cirrus is formed at the end of each dorsal kinety. All features confirm the stability of the morphogenetic process in the genus.

Familial assignment and taxonomic challenges of *Strongylidium*, *Hemiamphisiella* and *Pseudouroleptus*

The familial assignment of *Strongylidium* has gone through a complicated history since the genus was established by Sterki (1878) with *S. crassum* Sterki, 1878 as the type species. Gelei (1929) erected the family Spirofilidae for hypotrichs with distinctly spiralled or obliquely curved cirral rows, with *Spirofilum* (junior synonym of *Hypotrichidium* Ilowaisky, 1921) as the type genus. Kahl (1932) included all non-euplotid hypotrichs, including *Strongylidium*, in the family Oxytrichidae Ehrenberg, 1838 and suggested that *Strongylidium* was closely related to *Uroleptus* Ehrenberg, 1831. However, the ventral cirral rows in *Uroleptus* are a midventral complex with cirral pairs arranged in a zigzag pattern, consistent with urostylids (Berger, 2006) but different from the unpaired arrangement in *Strongylidium*. Hence, a close relationship between these two genera is unlikely, a conclusion reached by recent phylogenetic analyses (Chen *et al.*, 2013b, 2015; present paper). Corliss (1961) also classified *Strongylidium* in Oxytrichidae. In his discussion of the probable heterogeneity of Oxytrichidae, Spirofilidae was cited as a possible valid family name. In the same year, Fauré-Fremiet (1961) published a brief but important paper, in which he erected two new suborders: Stichotrichina and Sporadotrichina (order Stichotrichida and Sporadotrichida in the system of Lynn, 2008). Fauré-Fremiet (1961) also erected a new family, Strongylidae [emended by Tuffrau (1972) to Strongylidiidae], in the suborder Stichotrichina, with *Strongylidium* as the type genus. Later, Borror (1972) recognized the family Spirofilidae and considered Strongylidiidae a junior synonym. Lynn & Small (2002), Jankowski (2007) and Lynn (2008) followed this classification. Stiller (1975) accepted only Strongylidiidae. Corliss (1977, 1979), however, accepted both Spirofilidae and Strongylidiidae (including *Strongylidium*). Jankowski (1979) suggested new names for previously described taxa, elevated genera to family rank and proposed superfamilial changes. One superfamily was Strongylidioidea, containing the Strongylidiidae (with *Strongylidium* in it), and four monotypic families (Atractidae, Hypotrichidiidae, Microspirettidae and Spirofilopsidae), which he later abandoned (Jankowski, 2007).

Pseudouroleptus Hemberger, 1985 has been assigned to several families since its description. *Pseudouroleptus* was originally classified in Amphisiellidae Jankowski, 1979 by Hemberger (1985), which was accepted by Jankowski (2007). Later, *Pseudouroleptus* was transferred to Kahliellidae Tuffrau, 1979 by Tuffrau (1987) and treated as *incertae sedis* in Kahliellidae by Lynn (2008). It is widely accepted that kahliellids retain some parental cirral rows after division (Berger, 2011). However, this feature is absent in *Pseudouroleptus*, and therefore, the classification of *Pseudouroleptus* within Kahliellidae is incorrect. In the current phylogenetic analyses (Fig. 6), *Pseudouroleptus* sequences cluster with *Strongylidium* and *Hemiamphisiella*, rather than with *Kahliella*, the type genus of Kahliellidae, also rejecting the inclusion of *Pseudouroleptus* in Kahliellidae. Eigner (1997) assigned *Pseudouroleptus* to the sporadotrichid family Oxytrichidae, because it shows 'neokinetal 3' anlagen development: anlagen V and VI of both filial products originate from a V-shaped primordium. Berger (1999) assigned the type species *Pseudouroleptus caudatus* Hemberger, 1985 to Oxytrichidae, owing to the presence of dorsal kinety fragmentation, which differs significantly from Oxytrichidae *sensu* Eigner (1997). Recently, the other four species, originally assigned to *Pseudouroleptus* but with a different dorsal kinety pattern, were moved to the genus *Bistichella* by Berger (2008). Most recently, *Pseudouroleptus* was transferred to Spirofilidae by Chen *et al.* (2015).

In the present study, spirofilid taxa were scattered throughout the phylogenetic tree: *Hypotrichidium paraconicum*, species of the type genus, clustered in the large clade of oxytrichids, and *Stichotricha aculeata* was sister to 'core urostylids', while the *Strongylidium–Hemiamphisiella–Pseudouroleptus* group was sister to an assemblage of three oxytrichids, indicating that Spirofilidae is not monophyletic (Fig. 6). Based on the morphological and morphogenetic information, species of *Hypotrichidium*, the type genus of Spirofilidae, differs significantly from *Strongylidium* and *Pseudouroleptus* as follows: (1) body pyriform in outline, with the posterior end twisted helically toward the left vs. body usually more or less fusiform, with slightly spiral ventral rows; (2) buccal cavity deep and rather large, extending more than half, usually more than two-thirds of body length vs. buccal cavity narrow, usually extending less than one-third of body length; and (3) cirral pattern and formation mode (no merging or fixed cirral rows vs. left ventral cirral row formed

from three anlagen; Paiva & Silva-Neto, 2007; Chen *et al.*, 2013a, b; 2015). These differences, together with the phylogenetic data, argue against the inclusion of *Strongylidium* and *Pseudouroleptus* in Spirofilidae.

The family-level classification of *Hemiamphisiella* is also problematic. Foissner (1988) erected the genus as a member of the family Amphisiellidae. Subsequently, it was most often assigned to the amphisiellids (Eigner & Foissner, 1994; Petz & Foissner, 1996; Lynn & Small, 2002; Berger, 2008; Lynn, 2008). According to Eigner (1997, 1999), however, *Hemiamphisiella*, like *Pseudouroleptus*, belongs to Oxytrichidae because of the 'neokinetal 3' anlagen formation. Berger (2008) was uncertain about the proper systematic position of the genus. *Hemiamphisiella* forms a distinct cirral row that is reminiscent of the amphisiellid median cirral row. Yet, the type population of *Hemiamphisiella terricola*, like *P. caudatus*, has four dorsal kineties (dorsal kinety fragmentation possibly present). Eigner & Foissner (1994) studied the cell division of another population of *H. terricola*, which had, however, only three dorsal kineties showing no kinety fragmentation or dorsomarginal row. Given that dorsal kinety fragmentation is not confirmed for the type population of *H. terricola*, Berger (2008) tentatively retained *Hemiamphisiella* in amphisiellids.

Although *Hemiamphisiella* has been assigned to the amphisiellids, there are significant differences between *Amphisiella* Gourret & Roeser, 1888 (type genus of Amphisiellidae) and *Hemiamphisiella*, as follows: (1) the anterior part of the FVTA IV stays at the frontal portion and forms as a short cirral row instead of joining the final amphisiellid median cirral row vs. the anterior part of the FVTA IV migrates and merges into the final left ventral cirral row (a typical oxytrichid feature); and (2) no postoral ventral cirrus in *Amphisiella* vs. postoral ventral cirrus present in *Hemiamphisiella*. These differences are also consistent in the phylogenetic analyses; *Hemiamphisiella* was grouped with *Strongylidium* and *Pseudouroleptus*, far away from *Amphisiella* in the tree (Fig. 6), indicating that the assignment of *Hemiamphisiella* to Amphisiellidae should be questioned.

Reactivation of the family Strongylidiidae Fauré-Fremiet, 1961

Although *Strongylidium*, *Hemiamphisiella* and *Pseudouroleptus* have been placed in different families and even different orders, they resemble each other, as follows: (1) cells narrowed or tailed posteriorly and more or less twisted about main body axis; (2) three clearly differentiated frontal cirri, one buccal cirrus and one III/2 cirrus; (3) postoral ventral cirrus usually present; (4) pretransverse ventral and transverse cirri absent; (5) a mixed left ventral cirral row, with the anterior, middle and posterior parts of the rows being generated from anterior segments of FVTA VI and IV and the whole of FVTA V; (6) a short or long right ventral cirral row formed by the posterior fragment of FVTA VI; (7) one marginal cirral row on each side; (8) caudal cirri present; and (9) dorsomarginal kineties absent (Berger, 1999, 2011; Paiva & Silva-Neto, 2007; Chen et al., 2013b, 2015). The highly characteristic formation pattern of the mixed left ventral cirral row and the many shared morphological features are unlikely to be the product of convergent evolution. The phylogenetic trees show that *Strongylidium*, *Hemiamphisiella* and *Pseudouroleptus* group together with full support (ML/BI, 100/1.00). Considering the combination of shared distinctive morphological and morphogenetic features, together with the phylogenetic analyses, we propose that these genera share a common ancestor.

In 1961, Fauré-Fremiet erected Strongylidiidae and provided a brief definition: body twisted about main body axis, two ventral and two marginal cirral rows, and transverse cirri absent. In the most recent major revisions (Tuffrau & Fleury, 1994; Shi, 1999; Lynn & Small, 2002; Jankowski, 2007; Lynn, 2008), Strongylidiidae was treated as a junior synonym of Spirofilidae. Considering the morphological and morphogenetic data, together with the phylogenetic analyses, we propose to reactivate Strongylidiidae for *Hemiamphisiella*, *Pseudouroleptus* and *Strongylidium* and give an improved diagnosis.

Improved diagnosis: Hypotrichia with elongate body, usually distinctly narrowed posteriorly and slightly twisted about main body axis. Three enlarged frontal cirri; one buccal cirrus; usually one cirrus (= cirrus III/2) left of anterior portion of left ventral cirral row; postoral ventral cirrus present or lacking, originates from FVTA IV; pretransverse ventral and transverse cirri absent; a long left ventral cirral row composed of an anterior portion formed by the anteriorly migrating cirri of FVTA VI, a middle portion formed by the anterior-most cirrus/cirri of FVTA IV, and a posterior portion formed by FVTA V; a short or long right ventral cirral row formed by posterior fragment of FVTA VI; one marginal cirral row on each side; caudal cirri present; dorsal kinety fragmentation present or secondarily lost, and dorsomarginal kineties absent.

Type genus: Strongylidium Sterki, 1878.

Genera included: Strongylidium Sterki, 1878; *Hemiamphisiella* Foissner, 1988; *Pseudouroleptus* Hemberger, 1985.

Systematic position of Strongylidiidae

The formation pattern of the mixed left ventral cirral row of the Strongylidiidae is reminiscent of the amphisiellid median cirral row in some groups of the stichotrichid ciliates (Berger, 2008). Additionally, most species of *Strongylidium* and *Hemiamphisiella* have only three bipolar dorsal kineties (without dorsal kinety fragmentation or dorsomarginal kineties), like most of the stichotrichids (Berger, 2008, 2011). Therefore, there is likely to be a close relationship between the *Strongylidium–Hemiamphisiella–Pseudouroleptus* group and stichotrichids. In most systems, the three genera were assigned to Stichotrichida (Hemberger, 1985; Tuffrau, 1987; Lynn & Small, 2002; Jankowski, 2007; Berger, 2008; Lynn, 2008). However, the dorsal kinety fragmentation present in *Pseudouroleptus* indicates a closer relationship with oxytrichids, as proposed by Berger (1999). This relationship is also supported by the molecular data (Fig. 6).

Based on our investigation, we believe the highly characteristic formation pattern of the mixed left ventral cirral row shared by the *Strongylidium–Hemiamphisiella–Pseudouroleptus* group is unlikely to be the product of convergent evolution. Considering the molecular data, the relationship between these genera becomes more evident. *Hemiamphisiella* and *Strongylidium* probably share a common ancestor (dorsal kinety fragmentation present) with *Pseudouroleptus*. The relationship between *Strongylidium–Hemiamphisiella–Pseudouroleptus* and stichotrichids should be re-examined, as: (1) parts of the frontoventral cirral row were from different anlagen, but in the latter the anterior part of the FVTA IV formed as a short cirral row instead of joining the amphisiellid median cirral row, whereas it merged into the final left ventral cirral row in the former (typical of oxytrichids); that is, all the mixed cirral rows in stichotrichids originate from two, not three, FTVA, as in the *Strongylidium–Hemiamphisiella–Pseudouroleptus* group; and (2) there was no postoral ventral cirrus formed in stichotrichids, but it was present in *Hemiamphisiella*, *Strongylidium* and *Pseudouroleptus* (Berger, 1999, 2008; Paiva & Silva-Neto, 2007; Chen *et al.*, 2013b, 2015). We suggest that the mixed cirral row of *Strongylidium–Hemiamphisiella–Pseudouroleptus* is a convergent evolution with that of some stichotrichids. Although there are only three bipolar dorsal kineties in most *Strongylidium–Hemiamphisiella* species and stichotrichids, we deduce that the dorsal kinety fragmentation in *Hemiamphisiella* and *Strongylidium* was a secondary loss instead of a plesiomorphy. *Pseudouroleptus* is possibly an ancestral form of *Hemiamphisiella* and *Strongylidium*.

Strongylidiidae was placed as a sister branch to the assemblage of three dorsomarginalians (*Architricha indica* Gupta *et al.*, 2006, *Paraurostyla viridis* (Stein, 1859) Borror, 1972, and *Oxytricha granulifera* Foissner & Adam, 1983) in the phylogenetic tree (Fig. 6).

Oxytricha granulifera is a typical 18 frontal-ventral-transverse cirri hypotrich, and *Architricha indica* is a species of 18 frontal-ventral-transverse cirri hypotrichs with multiple right and left marginal cirral rows. *Paraurostyla viridis* is a species with numerous frontoventral cirri arranged in three to seven longitudinal rows and one marginal cirral row on each side. As explained by Berger (1999) and Castro et al. (2016), however, the population identified as *P. viridis* (AF508766) was not verified by a ciliate taxonomy specialist (no morphological information is available for the population), and its position in the clade, with *A. indica* and *O. granulifera* instead of with other *Paraurostyla* species, suggests that misidentification cannot be excluded. In addition, confusion between long ventral rows and internal extra right marginal rows is common when the specimens are not checked carefully. Considering the phylogenetic topology, *P. viridis* (AF508766) is sister to *A. indica*, indicating that it is probably a species with 18 frontal-ventral-transverse cirri and multiple marginal cirral rows.

With *Strongylidium*, *Hemiamphisiella* and *Pseudouroleptus* clustered together, Strongylidiidae formed a sister branch with a clade of three Dorsomarginalia ciliates (*O. granulifera*, *A. indica* and *P. viridis*) with moderate to strong support (ML/BI, 86/1.00), and further nested into other Dorsomarginalians, indicating the close relationship between Strongylidiidae and Dorsomarginalia. However, besides the moderate to high support of most nodes in Strongylidiidae and the three closely related Dorsomarginalians, some of the basal positions and branches within Oxytrichidae in both ML and BI analyses were not robust. Given the low nodal support, it is not appropriate to draw any further conclusions.

ACKNOWLEDGEMENTS

This work was supported by the Natural Science Foundation of China (project numbers: 31401963, 31772477, 31430077), the China Scholarship Council and King Saud University, Deanship of Scientific Research, College of Science Research Center. We would like to thank Professor Xiaozhong Hu (Ocean University of China), who critically read the drafts and gave many helpful suggestions. Our thanks are also given to Professor Xiaofeng Lin, Southern China Normal University, and Dr Jie Huang, Chinese Academy of Sciences, for ensuring institutional support for this research.

REFERENCES

Adl SM, Simpson AG, Lane CE, Lukeš J, Bass D, Bowser SS, Brown MW, Burki F, Dunthorn M, Hampl V, Heiss A, Hoppenrath M, Lara E, Le Gall L, Lynn DH, McManus H, Mitchell EA, Mozley-Stanridge SE, Parfrey LW, Pawlowski J, Rueckert S, Shadwick L, Shadwick L, Schoch CL, Smirnov A, Spiegel FW. 2012. The revised classification of eukaryotes. *The Journal of Eukaryotic Microbiology* **59:** 429–493.

Alekperov IK. 2005. *An atlas of free-living ciliates. (Classes Kinetofragminophora, Colpodea, Oligohymenophora, Polyhymenophora)*. Borcali, Baku, 310.

Berger H. 1999. Monograph of the Oxytrichidae (Ciliophora, Hypotrichia). *Monographiae Biologicae* **78:** 1–1080.

Berger H. 2006. Monograph of the Urostyloidea (Ciliophora, Hypotricha). *Monographiae Biologicae* **85:** 1–1304.

Berger H. 2008. Monograph of the Amphisiellidae and Trachelostylidae (Ciliophora, Hypotricha). *Monographiae Biologicae* **88:** 1–737.

Berger H. 2011. Monograph of the Gonostomatidae and Kahliellidae (Ciliophora, Hypotricha). *Monographiae Biologicae* **90:** 1–741.

Biernacka I. 1963. Die Protozoenfauna in Danziger Bucht II. Die Charakteristik der Protozoen in untersuchten Biotopen der Seekuste. *Polskie Archiwum Hydrobiologii* **11:** 17–75.

Borror AC. 1972. Revision of the order Hypotrichida (Ciliophora, Protozoa). *The Journal of Protozoology* **19:** 1–23.

Bourland WA. 2015. Morphology, ontogenesis and molecular characterization of *Atractos contortus* Vörösváry, 1950 and *Stichotricha aculeata* Wrzesniowskiego, 1866 (Ciliophora, Stichotrichida) with consideration of their systematic positions. *European Journal of Protistology* **51:** 351–373.

de Castro LA, Küppers GC, Fernandes NM, Schlegel M, Paiva Tda S. 2016. Ontogeny and molecular phylogeny of *Apoamphisiella vernalis* reveal unclear separation between genera *Apoamphisiella* and *Paraurostyla* (Protozoa, Ciliophora, Hypotricha). *PLoS ONE* **11:** e0155825.

Chen L, Liu W, Liu A, Al-Rasheid KA, Shao C. 2013a. Morphology and molecular phylogeny of a new marine hypotrichous ciliate, *Hypotrichidium paraconicum* n. sp. (Ciliophora, Hypotrichia). *The Journal of Eukaryotic Microbiology* **60:** 588–600.

Chen L, Lv Z, Shao C, Al-Farraj SA, Song W, Berger H. 2016. Morphology, cell division, and phylogeny of *Uroleptus longicaudatu*s (Ciliophora, Hypotricha), a species of the *Uroleptus limnetis* complex. *The Journal of Eukaryotic Microbiology* **63:** 349–362.

Chen L, Zhao X, Ma H, Warren A, Shao C, Huang J. 2015. Morphology, morphogenesis and molecular phylogeny of a soil ciliate, *Pseudouroleptus caudatus caudatus Hemberger*, 1985 (Ciliophora, Hypotricha), from Lhalu Wetland, Tibet. *European Journal of Protistology* **51:** 1–14.

Chen L, Zhao X, Shao C, Miao M, Clamp J. 2017. Morphology and phylogeny of two new ciliates, *Sterkiella sinica* sp. nov. and *Rubrioxytricha tsinlingensis* sp. nov. (Protozoa, Ciliophora, Hypotrichia) from north-west China. *Systematics and Biodiversity* **15:** 131–142.

Chen X, Miao M, Ma H, Shao C, Al-Rasheid KA. 2013b. Morphology, morphogenesis and small-subunit rRNA gene sequence of the novel brackish-water ciliate *Strongylidium orientale* sp. nov. (Ciliophora, Hypotrichia). *International Journal of Systematic and Evolutionary Microbiology* **63:** 1155–1164.

Corliss JO. 1961. *The ciliated protozoa: characterization, classification, and guide to the literature*. Oxford, London, New York, Paris: Pergamon Press.

Corliss JO. 1977. Annotated assignment of families and genera to the orders and classes currently comprising the Corlissian scheme of higher classification for the phylum Ciliophora. *Transactions of the American Microscopical Society* **96:** 104–140.

Corliss JO. 1979. *The ciliated protozoa. Characterization, classification and guide to the literature*, *2nd edn*. Oxford, New York, Toronto, Sydney, Paris, Frankfurt: Pergamon Press.

Dong J, Lu X, Shao C, Huang J, Al-Rasheid KA. 2016. Morphology, morphogenesis and molecular phylogeny of a novel saline soil ciliate, *Lamtostyla salina* n. sp. (Ciliophora, Hypotricha). *European Journal of Protistology* **56:** 219–231.

Dragesco J, Dragesco-Kernéis A. 1986. Ciliés libres de l'Afrique intertropicale. Introduction à la connaissance et à l'étude des ciliés. *Faune Tropicale* **26:** 1–559.

Eigner P. 1997. Evolution of morphogenetic processes in the Orthoamphisiellidae n. fam., Oxytrichidae, and Parakahliellidae n. fam., and their depiction using a computer method (Ciliophora, Hypotrichida). *Journal of Eukaryotic Microbiology* **44:** 553–573.

Eigner P. 1999. Comparison of divisional morphogenesis in four morphologically different clones of the genus *Gonostomum* and update of the natural hypotrich system (Ciliophora, Hypotrichida). *European Journal of Protistology* **35:** 34–48.

Eigner P, Foissner W. 1994. Divisional morphogenesis in *Amphisiellides illuvialis* n. sp., *Paramphisiella caudate* (Hemberger) and *Hemiamphisiella terricola* Foissner, and redefinition of the Amphisiellidae (Ciliophora, Hypotrichida). *Journal of Eukaryotic Microbiology* **41:** 243–261.

Fauré-Fremiet E. 1961. Remarques sur la morphologie comparée et la systématique des ciliata Hypotrichida. *Académie des Sciences* **252:** 3515–3519.

Foissner W. 1982. Ökologie und Taxonomie der Hypotrichida (Protozoa: Ciliophora) einiger österreichischer Böden. *Archiv fü Protistenkunde* **126:** 19–143.

Foissner W. 1987. Neue und wenig bekannte hypotriche und colpodide Ciliaten (Protozoa: Ciliophora) aus Böden und Moosen. *Zoologische Beträge Neue Folge* **31:** 187–282.

Foissner W. 1988. Gemeinsame Arten in der terricolen Ciliatenfauna (Protozoa: Ciliophora) von Australien und Afrika. *Stapfia* **17:** 85–133.

Gao F, Warren A, Zhang Q, Gong J, Miao M, Sun P, Xu D, Huang J, Yi Z, Song W. 2016. The all-data-based evolutionary hypothesis of ciliated protists with a revised classification of the phylum Ciliophora (Eukaryota, Alveolata). *Scientific Reports* **6**, 24874.

Gelei J, 1929. Ein neuer Typ der hypotrichen Infusorien aus der Umgebung von Szeged. *Spirofilum tisiae* n. sp., n. gen., n. fam. *Archiv für Protistenkunde* **65:** 165–182.

Hemberger H. 1985. Neue Gattungen und Arten hypotricher Ciliaten. *Archiv für Protistenkunde* **130:** 397–417.

Huang J, Luo X, Bourland WA, Gao F, Gao S. 2016. Multigene-based phylogeny of the ciliate families Amphisiellidae and Trachelostylidae (Protozoa: Ciliophora: Hypotrichia). *Molecular Phylogenetics and Evolution* **101:** 101–110.

Jankowski AW. 1979. Revision of the order Hypotrichida Stein, 1859 (Protozoa, Ciliophora). Generic catalogue, phylogeny, taxonomy. *Trudy Zoologischeski Institute Leningrad* **86:** 48–85 (in Russian with English summary).

Jankowski AW. 2007. Phylum Ciliophora Doflein, 1901. In: Alimov AF, ed. *Protista. Part 2. Handbook on zoology*. St. Petersburg: Russian Academy of Sciences, Zoological Institute, 371–993 (in Russian with English summary).

Kahl A. 1932. Urtiere oder Protozoa I: Wimpertiere oder Ciliata (Infusoria) 3. Spirotricha. *Tierwelt Deutschlands* **25:** 399–650.

Kumar S, Bharti D, Quintela-Alonso P, Shin MK, La Terza A. 2016. Fine-tune investigations on three stylonychid (Ciliophora, Hypotricha) ciliates. *European Journal of Protistology* **56:** 200–218.

Li F, Lyu Z, Li Y, Fan X, Al-Farraj SA, Shao C, Berger H. 2017. Morphology, morphogenesis, and molecular phylogeny of *Uroleptus* (*Caudiholosticha*) *stueberi* (Foissner, 1987) comb. nov. (Ciliophora, Hypotricha), and reclassification of the remaining *Caudiholosticha* species. *European Journal of Protistology* **59:** 82–98.

Li L, Zhao X, Ji D, Hu X, Al-Rasheid KA, Al-Farraj SA, Song W. 2016. Description of two marine amphisiellid ciliates, *Amphisiella milnei* (Kahl, 1932) Horváth, 1950 and *A. sinica* sp. nov. (Ciliophora: Hypotrichia), with notes on their ontogenesis and SSU rDNA-based phylogeny. *European Journal of Protistology* **54:** 59–73.

Luo X, Fan Y, Hu X, Miao M, Al-Farraj SA, Song W. 2016. Morphology, ontogeny, and molecular phylogeny of two freshwater species of *Deviata* (Ciliophora, Hypotrichia) from Southern China. *The Journal of Eukaryotic Microbiology* **63:** 771–785.

Luo X, Gao F, Yi Z, Pan Y, Al-Farraj SA, Warren A. 2017. Taxonomy and molecular phylogeny of two new brackish hypotrichous ciliates, with the establishment of a new genus (Ciliophora, Spirotrichea). *Zoological Journal of the Linnean Society* **179:** 475–491.

Lynn DH. 2008. *The ciliated Protozoa: characterization, classification, and guide to the literature*, *3rd edn*. New York: Springer.

Lynn DH, Small EB. 2002. Phylum Ciliophora. In: Lee JJ, Leedale GF, Bradbury P, eds. *An illustrated guide to the Protozoa, 2nd edn. Organisms traditionally referred to as Protozoa, or newly discovered groups*, **Vol. I**. Lawrence: Society of Protozoologists, 371–656.

Medlin L, Elwood HJ, Stickel S, Sogin ML. 1988. The characterization of enzymatically amplified eukaryotic 16S-like rRNA-coding regions. *Gene* **71:** 491–499.

Miller MA, Pfeiffer W, Schwartz T. 2010. Creating the CIPRES Science Gateway for inference of large phylogenetic trees. In *Proceedings of the Gateway Computing Environments Workshop (GCE)*, 14 Nov. New Orleans, LA: Institute of Electrical and Electronics Engineers, 1–8.

Nylander JA. 2004. *MrModeltest*. Evolutionary Biology Centre, Uppsala University.

Paiva TS, Silva-Neto ID. 2007. Morphology and morphogenesis of *Strongylidium pseudocrassum* Wang and Nie, 1935, with redefinition of *Strongylidium* Sterki, 1878 (Protista: Ciliophora: Stichotrichia). *Zootaxa* **1559:** 31–57.

Pan X, Bourland WA, Song W. 2013. Protargol synthesis: an in-house protocol. *The Journal of Eukaryotic Microbiology* **60:** 609–614.

Park KM, Jung JH, Min GS, Kim S. 2017. *Pseudonotohymena antarctica* n. g., n. sp. (Ciliophora, Hypotricha), a new species from Antarctic soil. *The Journal of Eukaryotic Microbiology* **64:** 447–456.

Petz W, Foissner W. 1996. Morphology and morphogenesis of *Lamtostyla edaphoni* Berger and Foissner and *Onychodromopsis flexilis* Stokes, two hypotrichs (Protozoa: Ciliophora) from Antarctic soils. *Acta Protozoologica* **35:** 257–280.

Ronquist F, Teslenko M, van der Mark P, Ayres DL, Darling A, Höhna S, Larget B, Liu L, Suchard MA, Huelsenbeck JP. 2012. MrBayes 3.2: efficient Bayesian phylogenetic inference and model choice across a large model space. *Systematic Biology* **61:** 539–542.

Sela I, Ashkenazy H, Katoh K, Pupko T. 2015. GUIDANCE2: accurate detection of unreliable alignment regions accounting for the uncertainty of multiple parameters. *Nucleic Acids Research* **43:** W7–W14.

Shi X. 1999. Systematic revision of the order Hypotrichida I. Protohypotrichina and Stichotrichina (Ciliophora). *Acta Zootaxonomica Sinica* **24:** 241–264 (in Chinese with English summary).

Stamatakis A. 2014. RAxML version 8: a tool for phylogenetic analysis and post-analysis of large phylogenies. *Bioinformatics (Oxford, England)* **30:** 1312–1313.

Sterki V. 1878. Beiträge zur Morphologie der Oxytrichinen. *Zeitschrift für wissenschaftliche Zoologie* **31:** 29–58.

Stiller J. 1975. Die familie Strongylidiidae Fauré-Fremiet, 1961 (Ciliata: Hypotrichida) und Revision der Gattung *Hypotrichidium* Ilowaisky, 1921. *Acta Zoologica Hungarica* **21:** 221–231.

Tamura K, Stecher G, Peterson D, Filipski A, Kumar S. 2013. MEGA6: molecular evolutionary genetics analysis version 6.0. *Molecular Biology and Evolution* **30:** 2725–2729.

Tucolesco J. 1962. Protozoaires des eaux souterraines. I. 33 espèces nouvelles d'infusoires des eaux cavernicoles roumaines. *Annales de Spéléologie* **17:** 89–105.

Tuffrau M. 1972. Caractères primitifs et structures évoluées chez les Ciliés hypotriches: le genre *Hypotrichidium*. *Protistologica* **8:** 257–266.

Tuffrau M. 1987. Proposition d'une classification nouvelle de l'ordre Hypotrichida (Protozoa, Ciliophora), fondées récentes. *Annales des sciences naturelles (Zoologie et biologie animale)* **13:** 111–117.

Tuffrau M, Fleury A. 1994. Classe des Hypotrichea Stein, 1859. In: De Puytorac P, ed. *Traité de Zoologie, Infusoires Ciliés*. **Vol. 2**. Paris: Masson, 83–151.

Wang C, Nie D. 1932. A survey of the marine protozoa of Amoy. Contributions from the marine biological association of China. *Zoological Series* **8:** 285–385.

Wang C, Nie D. 1935. Report on the rare and new species of fresh-water infusoria, part II. *Sinensia* **6:** 399–524.

Wang J, Lyu Z, Warren A, Wang F, Shao C. 2016. Morphology, ontogeny and molecular phylogeny of a novel saline soil ciliate, *Urosomoida paragiliformis* n. sp. (Ciliophora, Hypotrichia). *European Journal of Protistology* **56:** 79–89.

Wilbert N. 1975. Eine verbesserte Technik der Protargolimprägnation für Ciliaten. *Mikrokosmos* **64:** 171–179.

Zhao X, Gao S, Fan Y, Strueder-Kypke M, Huang J. 2015. Phylogenetic framework of the systematically confused *Anteholosticha–Holosticha* complex (Ciliophora, Hypotrichia) based on multigene analysis. *Molecular Phylogenetics and Evolution* **91:** 238–247.